Comparison of the cellular and biochemical properties of Plasmodium falciparum choline and ethanolamine kinases

Blandine Alberge, Leila Gannoun-Zaki, Céline Bascunana, Christophe Tran van Ba, Henri Vial, Rachel Cerdan

TITLE

Comparison of the cellular and biochemical properties of *Plasmodium falciparum* choline and ethanolamine kinases.

Author names

Blandine ALBERGE[*], Leila GANNOUN-ZAKI[*], Céline BASCUNANA[†], Christophe TRAN VAN BA[*], Henri VIAL[*,1] and Rachel CERDAN[*,1]

[*] Laboratoire de Dynamique des Interactions Membranaires Normales et Pathologiques (DIMNP) Universités de Montpellier II et I, Centre National de la Recherche Scientifique (CNRS), UMR 5235, Montpellier, F-34095, France.

† Present address: Laboratoire d'Ingénierie Cellulaire et Biotechnologique, CEA/DSV/IBEB/SBTN, CEA Marcoule BP 17171 Bagnols sur Cèze, F-30 207, France.

[1] To whom correspondence should be addressed (email rachel.cerdan@univ-montp2.fr or vial@univ-montp2.fr)

Short Title:

Choline and ethanolamine kinases of *Plasmodium falciparum*

Key words:

Plasmodium falciparum, choline kinase, ethanolamine kinase, phospholipid metabolism, kinetic parameter, inhibition

Abbreviations used:

PL, phospholipid; Cho, choline; ethanolamine, Etn; Ser, serine; CDP-Etn, CDP-ethanolamine; CDP-Cho, CDP-choline; *Pf*EK, *P. falciparum* ethanolamine kinase; *Pf*CK, *P. falciparum* choline kinase; PtdEtn, phosphatidylethanolamine; PtdCho, phosphatidylcholine; *Pf*CEPT, *P. falciparum* choline/ethanolamine phosphotransferase; *Pf*ECT, *P. falciparum* CTP:phosphoethanolamine cytidylyltransferase; *Pf*CCT, *P. falciparum* CTP:phosphocholine cytidylyltransferase; RBC, red blood cell; IRBC, infected red blood cell; NIRBC, non-infected red blood cell; HC-3, hemicholinium-3; 2-AB, 2-amino 1-butanol.

ABSTRACT

The proliferation of the malaria-causing parasite *Plasmodium falciparum* within the erythrocyte is concomitant with massive phosphatidylcholine and phosphatidylethanolamine biosynthesis. Based on pharmacological and genetic data, *de novo* biosynthesis pathways of both phospholipids appear essential for parasite survival. The present study characterizes *P. falciparum* choline kinase (*Pf*CK) and ethanolamine kinase (*Pf*EK), which catalyse the first enzymatic steps of these essential metabolic pathways. Recombinant *Pf*CK and *Pf*EK were expressed as His-tagged fusion proteins from over-expressing *E. coli* strains, then purified to homogeneity and characterized. Using mice-polyclonal antibodies against recombinant kinases, *Pf*CK and *Pf*EK were shown to be localized within the parasite cytoplasm. Protein expression levels increased during erythrocytic development. *Pf*CK and *Pf*EK appeared specific to their respective substrate and followed Michaelis-Menten kinetics. The K_m value of *Pf*CK for choline was 135.3 ± 15.5 µM. *Pf*CK was also able to phosphorylate ethanolamine with a very low affinity. *Pf*EK was found to be an ethanolamine-specific kinase (K_m = 475.7 ± 80.2 µM for ethanolamine). The quaternary ammonium Hemicholinium-3 and an ethanolamine analog, 2-amino 1-butanol selectively inhibited *Pf*CK or *Pf*EK. In contrast, the bisthiazolium compound T3 designed as a choline analog and currently in clinical trials for antimalarial treatment, affected similarly *Pf*CK and *Pf*EK activities. Inhibition exerted by T3 was competitive for both *Pf*CK and *Pf*EK and correlated with the impairment of cellular phosphatidylcholine biosynthesis. Comparative analyses of sequences and structures between both kinase types gave insights into their specific inhibition profiles and into the dual capacity of T3 to inhibit both *Pf*CK and *Pf*EK.

INTRODUCTION

Plasmodium falciparum, the parasite of most severe forms of human malaria, requires intense membrane neogenesis to achieve successful growth and proliferation inside its hosts. During pathogenic blood development, one of the drastic changes is a six-fold increase in the content of phospholipids (PL) with a quasi-absence of cholesterol [1, 2]. Since PL salvage from the host plasma is not significant, the prodigious proliferative capacity of malaria parasite relies on its own biosynthetic machinery, more particularly on the synthesis of phosphatidylcholine (PtdCho) and phosphatidylethanolamine (PtdEtn) which represent 75 to 85% of the total parasitic PL content [3, 4]. Like other eukaryotic cells, *Plasmodium* is capable of synthesizing PtdCho and PtdEtn *via* the *de novo* CDP-choline and CDP-ethanolamine (Kennedy) pathways and a CDP-DAG dependent pathway leading to phosphatidylserine which can be decarboxylated into PtdEtn. In addition, a newly identified plant-like pathway involving serine decarboxylase and phosphoethanolamine N-methyltransferase generates additional PtdCho and PtdEtn in the parasite [5-7].

Parasite-driven lipid synthesis accompanying parasite growth has been shown to be essential and many steps within PL metabolism offer potential targets for chemotherapy [8, 9]. Because the intraerythrocytic parasite relies on host-imported precursors, the use of commercial choline (Cho) or ethanolamine (Etn) analogs identified the *de novo* PtdCho and PtdEtn metabolic pathways as vital to the parasite blood stage [9, 10]. Unquestionably, the most advanced approach is through the use of Cho analogs possessing one or two quaternary ammoniums. Indeed, we have identified Cho analogs that inhibit *P. falciparum* asexual blood stages at single digit nanomolar concentrations [11, 12]. The bisthiazolium T3 [13] is currently in development for severe malaria in human clinical trials. The primary mechanism of T3 antimalarial activity is likely *via* the perturbation of an organic cation transporter that mediates Cho entry into infected erythrocytes [14], thereby preventing the first crucial step in *de novo* PtdCho biosynthesis [13]. The development of Cho analogs as innovative antimalaria therapeutics proves that targeting lipid metabolism is a viable approach.

An alternative pharmacological strategy consists in interfering with enzymatic steps in the essential metabolic pathways for parasite lipid formation. In the so-called Kennedy pathway, Cho diverted from the host is phosphorylated by choline kinase (CK) into phosphocholine (P-Cho) which is subsequently coupled to CTP, thus generating CDP-Cho by a CTP-phosphocholine cytidylyltransferase (CCT). An equivalent *de novo* pathway exists for *Plasmodium* PtdEtn synthesis implying an ethanolamine kinase (EK) as first enzymatic step. In *Plasmodium*, the CDP-activated polar head groups are converted into the final products

PtdCho and PtdEtn by a common parasite choline/ethanolamine phosphotransferase (CEPT) [15] in presence of diacylglycerol (supp. Figure 1). Recent genetic experiments in the rodent malaria parasite *P. berghei* indicate that the genes coding for CK, CCT, CTP: phosphoethanolamine cytidylyltransferase (ECT) and CEPT are essential for parasite survival (Déchamps and Vial, personal communication), thus identifying enzymes involved in *de novo* PtdCho and PtdEtn metabolic pathways as potential targets for novel antimalaria therapy.

This study aims at characterizing *P. falciparum* CK (*Pf*CK) (EC 2.7.1.32) and EK (*Pf*EK) (EC 2.7.1.82) which catalyze the first committed step for *de novo* PtdCho and PtdEtn synthesis, respectively, phosphorylating the plasma-originating Cho and Etn (Supp. Figure 1). In mammalian cells, CK is considered as the connection between PL metabolism and cell cycle regulation [16]. Increasing interest in CK arose from the involvement of human α-isoform CK in cell proliferation regulation and carcinogenesis [16-18]. High levels of PtdCho resulting from an up-regulation of genes coding for Cho transporter and for CK correlate as a biochemical marker of breast cancer [19] while CKα depletion selectively kills many tumor-derived cell lines [20-22]. Antitumoral strategy targeting this enzyme and rational drug design are currently actively investigated [23-27].

P. falciparum at the blood stage likely possesses two distinct proteins for the phosphorylation of Cho and Etn with specificity for their natural substrate in parasite lysates [28] and the recombinant *Pf*CK (PlasmoDB: PF14_0020) has been characterized *in vitro* [29, 30]. A putative EK is annotated in the genome of all *Plasmodium* species (PlasmoDB: PF11_0257) (http://PlasmoDB.org) [31] but its activity has not been identified and characterized yet. This work identifies the activity of the gene product PF11_0257 as *P. falciparum* EK. A comparative study of *Pf*CK and *Pf*EK is presented for both their cellular expression and their properties as recombinant proteins with the characterization of their substrate requirements as well as their selective inhibition. Interestingly, we found that the bisthiazolium T3, currently developed as a choline analog for malaria therapy, equally inhibited both enzymatic activities while specifically impairing parasite PtdCho biosynthesis.

EXPERIMENTAL

Parasite culture and cDNA synthesis

The *P. falciparum* 3D7 strain was maintained in A+ or O+ human red blood cells (RBC) (Etablissement Français du Sang, Pyrénées Méditerannée) at 5% hematocrit in RPMI 1640 medium (Gibco) supplemented with 25 mM HEPES, 0.11 mM hypoxanthine and 0.5% (w/v) Albumax II (Gibco). Synchronisation of parasite cultures was performed twice at 36 hours interval using 5% sorbitol in phosphate buffered saline (PBS) for 5 min at 37° C during two parasite life cycles [32]. Infected erythrocytes were lysed by 0.1 % saponin in cold PBS at 4° C. After centrifugation at 1300×g for 5 min, the pellet of free parasites was washed twice with cold PBS. Genomic DNA was isolated from free parasites using the QIAamp® DNA Blood Mini kit (Qiagen) according to the manufacturer's instructions. Total RNA was extracted from infected RBC (IRBC) using the RNAaqueous^{TM} kit (Ambion) and cDNA was obtained by RT-PCR (SuperScript^{TM} III First-Strand Synthesis SuperMix, Invitrogen).

Cloning, Over-expression and Purification of PfCK and PfEK

The primary sequences of the full-length *Pf*CK (440 amino-acids) and putative *Pf*EK (423 amino-acids) were identified from PlasmoDB (http://PlasmoDB.org) [31]. The two ORFs were amplified by PCR from *P. falciparum* cDNA, using the high-fidelity Phusion polymerase with the forward primers 5'-CAA**GCTAGC**ATGGAAAGCAAAATCTGTGACC-3', 5'-CAA**GCTAGC**ATGGAATATCAACTAAGAGAAATTGATG-3' and the reverse primers, 5'-CAA**CTCGAG**ATCGTCATAATCCTTGATAATATTTTTG-3', 5'-CAA**CTCGAG**GTTTTTTTCCAATTTGCTCCTAAATTTTAC-3', respectively for *Pf*CK and *Pf*EK. Restriction sites NheI and XhoI are shown in bold. PCR fragments were ligated by T4 DNA ligase (BioLabs) into pET24b vector, to produce pET24b-*Pf*CK and pET24b-*Pf*EK for inducible expression of C-terminal hexahistidine-tagged recombinant proteins. All constructs were controlled by sequencing. The plasmids were transformed into *E.coli* strain BL21(DE3)pRIL. Bacteria were grown in LB medium containing 40 µg/ml chloramphenicol and 50 µg/ml kanamycin at 37° C. Expression of the recombinant proteins was induced by the addition of 0.5 mM isopropyl β-D-thiogalactopyranose (Invitrogen). Cultures were incubated for 5h at 28°C. After centrifugation (15 min at 3000×g), cells were suspended in 10 ml of lysis buffer (25 mM Tris-HCl, pH 8.0, 2mM β-mercapto-ethanol, 0.2 mM phenylmethylsulfonyl fluoride) containing one protease inhibitor cocktail tablet (Complete

Mini, EDTA-free, Roche). Lysis was performed by three passages through a French press (Thermo Spectronic), at a pressure of 1000 Pascal. Supernatants were isolated after centrifugation at 14000×g for 30 min at 4°C. For the first step of *Plasmodium* recombinant protein purification, the supernatant was loaded onto a 1ml HisTrap chelating column (GE Healthcare). After washing steps, the recombinant *Pf*CK and *Pf*EK were eluted with 250 mM imidazole. Imidazole was removed on desalting PD10 column (GE Healthcare), and the Ni-NTA purified proteins were concentrated using Amicon Ultra-15 (Millipore) to a final volume ~1ml. The kinases were further purified on a S75 (for *Pf*CK) or on a S200 (for *Pf*EK) gel filtration sepharose column (HiLoad Superdex, GE Healthcare) in 0.15 M NaCl, 25 mM Tris-HCl, pH 8.0 buffer and 2 mM β-mercapto-ethanol at a flow rate of 1 ml/min. Protein concentrations were determined by the Bradford method [33] with bovine serum albumin (Pierce) as standard. Purification steps were followed by SDS - polyacrylamide gel electrophoresis.

Circular Dichroism analysis

Purified recombinant proteins (concentrated at 0.3 mg/ml) were used for UV-CD analysis in 20mM sodium phosphate, pH 7.4 buffer and 2mM β-mercapto-ethanol. CD spectra were recorded from 180 to 260 nm at 20° C on a Chirascan Circular Dichroism Spectrophotometer (Applied Photophysics Inc.) with a 0.5 cm path-length quartz cell. Data were collected at 0.5 nm intervals and an accumulation time of 1s. All protein spectra were measured three times and corrected by subtraction of respective buffer spectra. The *Pf*CK and *Pf*EK spectra were analysed with CDNN CD Spectra Deconvolution Software (Applied Photophysics).

Antibody production and Western immunoblotting

Eight-week-old female BALB/c mice (Charles River laboratories, France) were immunized by subcutaneous injections of 20 to 50 µg of purified recombinant *Pf*CK or *Pf*EK emulsified in Freund adjuvant and boosted every three weeks by two successive injections. For Western blots, IRBC were lyzed and free parasites were obtained as described in *Parasite culture* section. Parasite extracts were separated using 12% SDS-PAGE under reducing conditions and transferred onto a nitrocellulose membrane (Protran, Whatman). Equivalent amount of cells were loaded in each well (1×10^7 cells/well). Membranes were incubated either with pre-immune or immune mice sera (1:500 dilution for anti-*Pf*CK and 1:2,500 dilution for anti-*Pf*EK), then with horseradish peroxidase conjugated anti-mouse IgG (Promega). Signals were

detected by chemioluminescence (ECL Western Blotting Detection Reagents, GE Healthcare).

Immunofluorescence assays

IRBC fixed in 4% para-formaldehyde and permeabilized by 0.1% Triton X-100 for 10 min, were incubated with anti-*Pf*CK (1:100 dilution) or anti-*Pf*EK (1:200 dilution) antibodies overnight at 4° C. The presence of *Pf*CK or *Pf*EK was revealed by incubation with goat anti-mouse IgG green Alexa Fluor 488 (Invitrogen) for 1 h at room temperature. Cells were plated on 10 well-slides then mounted on slides using a Vectashield mounting medium containing diamidino phenylindole (DAPI) (Vector Laboratories, Inc.). Parasites were visualized with an upright AxioImager-Z1 microscope equipped with an apotome and differential interference contrast for transmitted light (Carl Zeiss Inc.). Images were acquired using a ×63, 1.4 apochromat oil-objective. Cropping and brightness/contrast adjustments were performed with Axiovision (Carl Zeiss Inc.) and ImageJ (MacBiophotonics) softwares.

Kinetic parameters and inhibition assays for PfCK and PfEK

Recombinant *Pf*CK and *Pf*EK were incubated with [methyl-^{14}C] choline or [2-^{14}C] ethan-1-ol-2-amine with specific activity of 56 µCi/µmol or 55 µCi/µmol, respectively (Amersham Biosciences). The enzymatic activities were measured by the formation of radio-labeled phosphocholine and phosphoethanolamine. Assays were adapted from the optimization in *Plasmodium*-infected homogenates [28, 34]. Enzymatic reactions were carried out with 125 mM Tris-HCl, pH 8.0 buffer, 10 mM ATP, 5 mM EGTA, 10 mM $MgCl_2$ and 0.25 µCi of radio-labelled precursors for each assay in a final volume of 100 µl. Reactions were initiated with the addition of 0.5 µg of *Pf*CK or 2 µg *Pf*EK followed by 5 or 10 min incubation at 37°C for *Pf*CK or *Pf*EK, respectively. Reactions were stopped by heating at 96°C for 5 min. For each assay, a sample of 20 µl was spotted onto a thin layer chromatography (TLC) silica-gel plate, previously activated at 100°C for 1 h. Radio-labelled products and substrates were then separated in a buffer containing ethanol/2% ammonia (1:1, v/v). Plates were exposed overnight to a storage phosphor screen (Molecular Biodynamics) then analyzed on a PhosphoImager (Storm 840, Amersham Biosciences). Radioactive spots identified by the migration of appropriate standards (P-Cho and P-Etn) were scraped directly into scintillation vials. Radioactivity was determined using a Beckman LS6500 liquid-scintillation spectrometer after the addition of 3ml of scintillant (Ultima Gold, Perkin Elmer).

For the inhibition assays, two commercial compounds, hemicholinium-3 (Sigma), 2-amino-1-butanol (Aldrich), and a bisthiazolium compound T3 were tested. Inhibition assays were performed on recombinant proteins and native *Pf*EK and *Pf*CK from *P. falciparum* extracts. Soluble parasite extracts were obtained after saponin treatment of synchronized IRBC cultures at the schizont stage (1×10^7 parasites). Parasite pellets were washed in cold PBS and lyzed by sonication (Digital Sonifier, Branson Ultrasonics Corporation). The soluble fraction was recovered after centrifugation at 14000×g. Inhibition assays were measured by using the substrate concentrations at their respective affinity (K_m value) and by varying the inhibitor concentrations. For the determination of the inhibition constant K_i of T3, different concentrations of inhibitor were used. Substrate or inhibitor dependent curves were analyzed using GraphPad Prism 4 (GraphPad software, Inc.) and were represented using the Michaelis-Menten equation or the Lineweaver-Burk double reciprocal plots for K_m, V_{max}, K_i determination.

Determination of the critical micellar concentration of T3 by light scattering

The critical micellar concentration of T3 was determined by following the signal of dynamic light scattering when diluting a highly concentrated T3 solution. All the assays were carried out in the buffer used for the inhibition assays (Tris-HCl, pH 8 buffer). The intensity of the Rayleigh scattering band (*R*) (in kilo counts per second) was measured for each T3 concentration. Measurements were done on a Zeta Nano Series (Malvern Instrument) and data processed according to the manufacturer recommendations with DTS program. The intercept between the two straight lines corresponded to the cmc value.

Inhibition of P. falciparum phosphatidylcholine and phosphatidylethanolamine biosynthesis.

The incorporations of radio-labelled [^{3}H] -Cho (20 µM, 0.5 Ci/mmol) or [^{3}H]-Etn (2 µM, 4.2 Ci/mmol) into PtdCho or PtdEtn and of [^{3}H]-hypoxanthine (1 µCi/well) into nucleic acids were measured on infected erythrocyte suspensions. Drug effects on *P. falciparum* growth were measured in 96 well microtiter plates filled in with 100 µl of *P. falciparum* IRBC suspension (3% final hematocrit and 5% parasitemia) and 50 µl of complete medium (choline-free RPMI 1640, 25mM Hepes, 10% human serum) with or without the drug. After 30 min incubation at 37°C, 50 µl of radio-labelled precursor was added to the suspensions. Parasite cultures were maintained for 3 hours at 37°C, and then frozen at -80°C. After

thawing, the parasite macromolecules, including radioactive nucleic acids and lipids, were retained on glass fiber filters (Perkin Elmer) (pre-treated with 0.05% polyethylene glycol for Cho incorporation). Radioactivity was counted after the addition of scintillation cocktail (Ultima Gold, Perkin Elmer) in a liquid scintillation spectrometer. Dose-response curves were analyzed using GraphPad Prism 4 (GraphPad software, Inc.). The results are expressed as the concentration of drug resulting in 50% inhibition (IC_{50}) of Cho, Etn or hypoxanthine incorporations into PC, PE or nucleic acids, respectively.

RESULTS

Sequence analysis of P. falciparum CK and putative EK

The sequence alignment of the *Pf*CK sequence with other known CKs exhibited three conserved motifs; (1) the ATP binding loop with the conserved residues (Ser/Thr)-Asn, (2) the Brenner's phosphotransferase motif and (3) the choline/ethanolamine kinase motif (supp. Figure 2). We focused the analysis on residues involved in the binding of the Cho or Etn moiety. The Cho/Etn kinase motif consisted in a consensus sequence described by Ayoyama *et al*., 2004 [35] and redefined as follows: hhDhExxxxNxxxxDhxNhhxE (h stands for large hydrophobic residue). Analysis of the X-ray 3D structures of the human and *C. elegans* CKs [36] and the mutational studies of *C. elegans* CK [37], indicated that three residues (Asp306, Gln308 and Asn311 in human CKα-2) belonging to the Brenner's motif were also involved in choline binding. These three residues are conserved in CK sequences including *Pf*CK. Moreover, the choline binding site consisted of a deep hydrophobic groove and an outer negatively charged surface as described for the human CK structure in complex with the phosphocholine product [36]. The hydrophobic interactions stabilizing the quaternary amine of choline were mediated by conserved aromatic residue (Tyr333, 354, 440 and Trp420, 423 in hCKα-2) [36]. All five residues were found at equivalent positions in the *Pf*CK sequence (supp. Figure 2).

The *P. falciparum* genome database PlasmoDB [31] predicted the presence of an intronless gene (PF11_0257) encoding a putative EK. The alignment of the putative *Pf*EK sequence with other EKs revealed the presence of the three conserved motifs already described for CKs (supp. Figure 2). The ATP binding loop and the Brenner's motif of putative *Pf*EK were highly similar to EK but also to CK sequences. The consensus sequence of the Cho/Etn kinase motif defined above was also present in putative *Pf*EK.

Over-expression, purification and circular dichroism analysis of recombinant PfCK and PfEK

We confirmed the coding sequence *of P. falciparum* EK by sequencing the cDNA of *P. falciparum* 3D7 strain (data not shown). The molecular mass of the deduced amino acid sequence was 49.9 kDa. DNA coding sequences of *Pf*CK and *Pf*EK were inserted into pET24b expression vector and expressed as C-terminal hexahistidine-tagged recombinant proteins in the *E. coli* strain BL21(DE3)pRIL. SDS-PAGE analysis of total proteins from IPTG-induced bacteria indicated the presence of prominent bands corresponding to the apparent molecular mass of approximately 50 and 48 kDa for *Pf*CK and *Pf*EK, respectively (supp. Figure 3A and 3B). Most of the recombinant proteins were found in the soluble fraction after bacterial lysis. Purification of each recombinant protein was performed first by a nickel-ion affinity chromatography. A further purification step using gel filtration chromatography yielded highly purified proteins as shown by the single detectable band on SDS-PAGE (supp. Figure 3C). The oligomerization states of both recombinant proteins were determined from the gel filtration elution profiles. The molecular mass obtained for *Pf*CK on a calibrated column was ~52 kDa, indicating that the protein was monomeric in 0.15 M NaCl, 20mM Tris, pH 8 buffer. In contrast, under the same conditions, *Pf*EK appeared dimeric with a molecular mass of ~109 kDa**.** Interestingly, *Pf*CK seemed to be the only monomeric CK [29] while all other characterized CK and EK were dimeric [35, 38-40]. The dimer interface, described for human and *C. elegans* CK crystal structures, comprised 16 residues located at the C-terminal of the ATP binding loop [36, 41] (supp. Figure 2). After the two purification steps, both purified proteins were recovered at a final concentration of around 0.3 mg/ml for further studies. Average yields at the end of the purification procedure were 8-10 mg of *Pf*EK and 1-2 mg of *Pf*CK per litre of bacterial culture. Circular dichroism (CD) was used to assess protein folding after the purification steps. Spectra clearly exhibited two local minima and a maximum at 190 nm characteristic of α-helix conformation (supp. Figure 3D). For both proteins, the CD spectra reflected folded proteins. Secondary structure content estimation gave approximately 30% and 40 % α-helix for *Pf*CK and *Pf*EK, respectively.

Cellular expression and localization of PfCK and PfEK

We generated specific antibodies against *Pf*CK and *Pf*EK recombinant proteins by immunization of BALB-c mice. The specificity of anti-*Pf*CK and anti-*Pf*EK antibodies was verified by Western blot analysis of parasite extracts. Only one band was detected at the expected molecular mass for both *Pf*CK and *Pf*EK, while pre-immune sera did not show any

significant signal (Figure 1A and 1B). The antibodies were then used to detect *Pf*CK and *Pf*EK at the different stages of parasite development (ring, trophozoite and schizont stages). *Pf*CK and *Pf*EK could not be detected by Western blot at the early stage (ring) (Figure 1C and 1D). At the trophozoite stage, anti-*Pf*CK detected a weak band while the band detected by anti-*Pf*EK was more intense (Figure 1C and 1D). At the end of the life cycle (schizont), both bands corresponding to *Pf*CK and *Pf*EK were more intense reflecting a maximal amount of both proteins at this stage of the *P. falciparum* blood development (Figure 1C and 1D). To localize both enzymes within the parasite, immunofluorescence analyses were carried out on non-synchronized parasite cultures. The signals of both anti-sera were spread throughout the parasite cytoplasm (Figure 2). Moreover, *Pf*CK and *Pf*EK were clearly detected at both mature stages (trophozoite and schizont) but also at the early ring stage (Figure 2), highlighting a greater sensitivity in the immunofluorescence assays with the anti-*Pf*CK and anti-*Pf*EK antibodies, compared to the Western blot analysis.

In vitro PfCK and PfEK assays revealed two distinct enzymatic activities

Enzymatic activities and associated kinetic parameters were determined for each purified recombinant protein. The assay conditions were adapted from the protocols optimized for extracts of *P. falciparum*-infected erythrocytes [28]. Enzymatic activities were measured by the formation of P-Cho or P-Etn from radio-labeled Cho or Etn, respectively. At the initial linear rate of the enzyme reactions, the activities of *Pf*CK and *Pf*EK were determined as substrate concentrations were increasing. The rate of catalysis described saturation curves reaching a plateau, characteristic of Michaelis-Menten kinetics for both recombinant enzyme activities (Figure 3). For *Pf*CK, Lineweaver-Burk plot analysis of the enzyme activity with Cho yielded a K_m value of 135.3 ±15.5 µM and a V_{max} value of 10.7 ± 2.8 µmol/min/mg (Figure 3A and Table 1). For *Pf*EK, the K_m value for Etn was 475.7 ±80.2 µM, revealing a weaker affinity of this kinase towards its substrate compared to *Pf*CK (Figure 3B). The specific activity of *Pf*EK for ethanolamine was determined to be 1.28 ±0.11 µmol/min/mg of recombinant *Pf*EK (Table 1). We evaluated the kinase selectivity by measuring their activities with swapped substrates. *Pf*CK was able to catalyze the phosphorylation of Etn, but the affinity was drastically decreased and the catalytic activity was found to be 62.2 ± 3.5 µmol/min/mg (approximately 6 times higher with Etn than with Cho as substrate) (Table 1 and supp. Figure 4). In contrast, *Pf*EK was not able to phosphorylate Cho (below a choline concentration to 1M). *Pf*EK was an ethanolamine-specific kinase.

Inhibition of PfCK and PfEK by selective compounds and by the antimalarial drug T3

The chemical structures of the *Pf*CK and *Pf*EK substrates differ by three methyl groups. Indeed, a quaternary ammonium in Cho replaces a primary amine in Etn. Due to the substrate-specificity of *Pf*CK and *Pf*EK, selective inhibition of the enzymatic activities was conceivable. On the basis of chemical properties of the substrates, Hemicholinium-3 (HC-3) and 2-amino 1-butanol (2-AB) were used as Cho and Etn analogs, respectively (Figure 4A). HC-3 has been reported to be an inhibitor of choline transport [42] and CK [43-45] while 2-AB was shown to specifically inhibit EK [28]. When added to the recombinant *Pf*CK, HC-3 dose-dependently inhibited the kinase activity. When Cho concentration was used at its K_m value, HC-3 significantly inhibited *Pf*CK from 0.1 mM, with the concentration of drug to inhibit half of the *in vitro Pf*CK activity (inhibition concentration 50: IC_{50}) of 0.58± 0.02 mM (Figure 4B). However, HC-3 was not able to significantly inhibit *Pf*EK below an inhibitor concentration of 3 mM (Figure 4C). Inversely, the Etn analog, 2-AB selectively inhibited *Pf*EK activity with IC_{50} value of 1.36± 0.17 mM but had no significant effect on *Pf*CK activity at this inhibitor concentration (IC_{50} value above 10 mM) (Figure 4B and 4C).

The bisthiazolium T3 (Figure 4A), designed as a Cho analog to target the PtdCho synthesis pathway [13, 46], was similarly assessed on the activity of both recombinant enzymes. T3 affected the activity of *Pf*CK through an inhibition effect reflected by an IC_{50} value of 1.12± 0.11 mM (Figure 4B). Remarkably, T3 dose-dependently inhibited the *Pf*EK activity at concentrations similar to those inhibiting *Pf*CK as evidenced by an IC_{50} value of 0.61± 0.02 mM (Figure 4C). While the substrate analogs of CK and EK activities selectively inhibited the recombinant *Pf*CK and *Pf*EK, T3 was able to equally inhibit *Pf*CK and *Pf*EK with comparable efficiency.

In addition, we investigated inhibitory properties of the compounds on *P. falciparum* endogenous *Pf*CK and *Pf*EK activities. 2-AB and HC-3 also selectively inhibited *Pf*EK and *Pf*CK activities, with respective IC_{50} of 0.46± 0.03 mM and 0.22± 0.01 mM (supp. Figure 5). The bis-thiazolium T3 inhibited both cellular activities within the same concentration range with IC_{50} of 0.79± 0.05 mM and 0.52± 0.03 mM, respectively (supp. Figure 5). T3 similarly inhibited recombinant and endogenous kinase activities as proved by comparable IC_{50} values. Thus, the inhibition specificities of 2-AB and HC-3 and the ability of T3 to inhibit both kinases were found on recombinant and endogenous EK and CK activities.

In order to elucidate the mode of action of T3, activity assays with increasing concentrations of drug were carried out on both recombinant *Pf*CK and *Pf*EK. Increasing concentrations of inhibitor augmented the slope of the primary plots (1/v=f(1/S)) and all lines intersect on the (1/v) axis (Figure 5A and 5B). T3 acted as a competitive inhibitor of Cho and Etn substrates. The K_i values of T3, calculated from Lineweaver-Burk linearization and the plot of the apparent K_m as a function of the inhibitor concentration, were found to be 1.03 mM for *Pf*CK and 0.73 mM for *Pf*EK (Figure 5A and 5B). These values indicated that T3 exerts a competitive inhibitory effect with similar affinity for both *Pf*CK and *Pf*EK. The Dixon plot of the reciprocal of velocity *vs* inhibitor concentration is also a convenient way of calculating the inhibition constant. Using this graph (not shown), we found comparable K_i values of T3 (0.9 and 0.7 mM for *Pf*CK and *Pf*EK, respectively) as those obtained from Lineweaver-Burk linearization. Taken together, these results indicated a competitive inhibition of T3 for both kinase reactions with K_i values in the same range as the IC_{50} values and an inhibitory effect of T3 affecting *Pf*CK and *Pf*EK activities with similar affinity.

As shown in figure 4A, T3 has two positively charged head groups linked by a hydrophobic hydrocarbon chain, properties resembling those of a cationic detergent. Although, T3 exerted a competitive inhibition on *Pf*CK and *Pf*EK activities, we wanted to exclude that T3 could affect the proteins in a detergent like manner. Thus, we determined the critical micellar concentration (cmc) value of T3 by dynamic light scattering. The measurements of the Rayleigh scattering band intensities (*R*) for various T3 concentrations were performed (supp. Figure 6). For low T3 concentrations, the intensity of the scattered light followed a linear correlation resulting from the presence of monomers in the solution. As the concentration of T3 increased, the equilibrium between the monomer and the micelle forms of T3 was reached as deduced from the abrupt increase of light intensity at the cmc. The cmc value of T3 was found to be at 200 mM in the buffer used for inhibition assays (Tris-HCl, pH 8) (supp. Figure 6). This value was far above the IC_{50} values of T3 found to inhibit *Pf*CK and *Pf*EK, excluding a detergent-like effect of the drug as the mechanism for the observed inhibition.

Effects of compounds on cellular phosphatidylcholine and phosphatidylethanolamine biosynthesis

We monitored newly synthesized PtdCho and PtdEtn of *P. falciparum* infected erythrocytes by measuring the incorporation rate of radio-labeled precursors. *P. falciparum* cultures were treated with the three compounds HC-3, AB-2 and T3. To detect unspecific effects, the incorporation of radio-labeled hypoxanthine into DNA was simultaneously evaluated. The

concentrations required to inhibit 50% of the DNA synthesis were found to be 74± 5 μM for T3 and above 2 mM for HC-3 and 2-AB.

HC-3 had a complete inhibitory effect on the Cho incorporation into cellular PtdCho with an IC_{50} value (concentration required to inhibit 50% of PtdCho synthesis) of 79± 9 μM (supp. Figure 7A). At this concentration, neither PtdEtn nor the DNA synthesis were yet altered (supp. Figure 7A). The production of PtdEtn was selectively decreased by AB-2 treatment (IC_{50} = 40± 4 μM) while this Etn analog did not affect PtdCho biosynthesis even when significantly higher concentrations were used (> 1 mM) (supp. Figure 7B). Thus, HC-3 and AB-2 exerted a selective effect on the *de novo* CDP-Cho and CDP-Etn biosynthesis pathways, respectively. When T3 was added to infected erythrocytes, the incorporation of Cho was impaired (IC_{50} = 12±3 μM) at concentrations that did not perturb DNA synthesis. In contrast, a decrease in PtdEtn synthesis was only observed at higher T3 concentrations that also affected hypoxanthine incorporation (supp. Figure 7C). Thus, the antimalarial effect of T3 is likely related to a decrease of parasite PtdCho but not PtdEtn synthesis.

DISCUSSION

This study provided evidence that the *P. falciparum* gene PF011_0257 coded for an ethanolamine kinase activity. We also showed that *Pf*EK and *Pf*CK were selective for their respective substrate, Etn and Cho. The catalysis of *Pf*CK toward the phosphorylation of Etn was probably of no physiological significance since both metabolic pathways appeared essential in *P. berghei* parasite indicating that one enzyme cannot be substituted to the other. The levels of both kinases increased within the cytoplasm along the parasite life cycle. This suggests that *Pf*CK and *Pf*EK could be dedicated to their own pathways, thereby increasing the possibilities for regulation processes.

As the Cho/Etn kinase motif did not exhibit any significant difference by comparing CK and EK sequences, we surmised that the specificity of these kinases resided elsewhere. Interestingly, the glutamine residue (Q_{290} for *Pf*CK and Q_{308} for hCKα-2) within the Brenner's motif, was conserved amongst the CKs while this position was occupied by a hydrophobic amino acid in EK sequences (supp. Figure 2). Ethanolamine-specific kinases lacked one of the five aromatic residues forming the hydrophobic pocket for the stabilization of the Cho quaternary amine (Y_{329} for *Pf*CK and Y_{354} for hCKα-2) [36]. Indeed, most CKs contained an insertion encompassing the Tyr329 located at the C-terminal end of the Cho/Etn motif (supp. Figure 2), which was not found in ethanolamine-specific kinases. Thus, within

the residues involved in the binding of the polar head substrate, CK sequences differed from EK sequences by the substitution of the pivotal polar residue of the Brenner's motif with a hydrophobic residue (Gln290 -> Leu298 for *Pf*CK and *Pf*EK) and by an insertion at the C-terminal of the Cho/Etn kinase motif of CKs. These observations were corroborated by the analysis of *S. cerevisiae* EK. This enzyme exhibited a polar residue (glutamine) where a hydrophobic residue is usually found (Leu298 for *Pf*EK). Moreover, *S. cerevisiae* EK sequence also contained the insertion at the C-terminal of the Cho/Etn kinase motif defined above as CK specific. To our knowledge, *Sc*EK is the only EK presenting significant Cho phosphorylation activity *in vitro* [16, 35, 39, 47, 48].

Since *Pf*CK and *Pf*EK discriminate their respective substrate containing a quaternary ammonium or a primary amine, selective inhibition by appropriate analogs is conceivable. The experiments reported here demonstrate that recombinant as well as endogenous *Pf*CK and *Pf*EK are selectively inhibited by two substrate analogs, HC-3 and 2-AB, respectively. Surprisingly, the antiphospholipid effector T3 designed as a Cho analog had an effect, not only on *Pf*CK activity but also on *Pf*EK activity. In order to obtain insights into the different inhibition profiles of HC-3 and 2-AB on one side and into the similar affinity of the bis-thiazolium for both enzymes on the other side, we carried out a combined analysis of sequence alignments and of kinase crystal structures. As we did for the comparison of CK and EK sequences (see above and supp. Figure 2), we exploited the 3D crystal structures of *Pf*CK and *P. vivax* EK (*Pf*EK structure being not available) recently solved by a structural genomics consortium. Although both kinase types share the same overall fold, an interesting difference appeared when both structures were superimposed. Indeed, the *Pf*CK crystal structure showed that the insertion comprising the tyrosine residue at the C-terminal of the Cho/Etn kinase motif was located near the catalytic site (Figure 6). As was evident in the primary sequence alignment, this insertion was absent in EK sequences. Additionally, the human CK crystal structure in complex with HC-3 revealed that one aromatic ring of HC-3 stacked onto the tyrosine ring residue of the insertion (Y_{354} for hCKα-2) (Figure 6). This CK-specific interaction could be indispensable to discriminate between the inhibitors and thus the substrates, whereas the absence of the insertion in *Pf*EK preventing any Tyr-mediated interaction would be detrimental for HC-3 or Cho binding. Similar affinities of T3 for both enzymes were observed. It is likely that the conformation of the thiazolium head group being planar contrary to Cho and HC-3 quarternary ammonium, allows its entry into the *Pf*EK catalytic site. Additionally, the flexibility due to the 12-carbon atom linker between both

thiazolium groups, could allow quaternary ammonia (or just one ammonium) to adapt to *Pf*CK and *Pf*EK catalytic sites.

More investigations are needed to explain the dual potentiality of T3 on both *Pf*CK and *Pf*EK activities. Since both metabolic pathways are essential, *Pf*CK and *Pf*EK appear crucial for the *P. falciparum* survival. In the parasite, T3 selectively impaired PtdCho biosynthesis that likely explains its antimalarial effect while PtdEtn biosynthesis did not appear to be primarily affected. As mentioned above, the primary action of T3 is likely to prevent Cho entry into the parasites by blocking an organic cation transporter. Nevertheless, the inhibition of two *Plasmodium* enzymes at similar levels opens the way to the design of new scaffolds toward dual molecules. The ability to affect more than one target for antimalarial therapy is precious to delay the emergence of resistant malaria strains, which is currently a crucial issue in the battle against malaria. 3D crystal structures of complexes between these both enzymes and T3 should provide the atomic details of the interactions, necessary for future structure-based drug design of novel analogs.

ACKNOWLEDGEMENTS:

We thank Dr. Martin Cohen-Gonsaud at the Centre de Biochimie Structurale in Montpellier for helpful discussions and help with circular dichroism experiments. We are grateful to Dr. Kai Wengelnik for helpful discussions and critical reading of this manuscript.

The *P. falciparum* 3D7 strain was obtained through the Malaria Research and Reference Reagent Resource Center (MR4).

FUNDING:

This work was supported by the European Union FP6 Network of Excellence BioMalPar LSHP-CT-2004-503578 and Integrated project Antimal [N° IP-018834].

REFERENCES:

1 Vial, H. and Ancelin, M. L. (1992) Malarial Lipids An overview. In Subcellular Biochemistry (Press, P., ed.), pp. 259-306, Avila, J. L. Harris, J. R., New York

2 Vial, H. J., Eldin, P., Tielens, A. G. M. and van Hellemond, J. J. (2003) Phospholipids in parasitic protozoa. Mol. Biochem. Parasitol. **126**, 143-154

3 Holz, G. G. (1977) Lipids and the malaria parasite. Bull. Wld. Hlth. Organiz (WHO) **55**, 237-248

4 Vial, H. and Ben Mamoun, C. (2005) Plasmodium Lipids: Metabolism and Function In Molecular Approach to Malaria. In Plasmodium Lipids: Metabolism and Function In Molecular Approach to Malaria (Sherman, I. W., ed.), pp. 327-352, ASM Press, Washington, DC

5 Elabbadi, N., Ancelin, M. L. and Vial, H. J. (1997) Phospholipid metabolism of serine in Plasmodium-infected erythrocytes involves phosphatidylserine and direct serine decarboxylation. Biochem. J. **324**, 435-445

6 Pessi, G., Choi, J. Y., Reynolds, J. M., Voelker, D. R. and Mamoun, C. B. (2005) In vivo evidence for the specificity of Plasmodium falciparum phosphoethanolamine methyltransferase and its coupling to the Kennedy pathway. J Biol Chem **280**, 12461-12466

7 Pessi, G., Kociubinski, G. and Ben Mamoun, C. (2004) A pathway for phosphatidylcholine biosynthesis in Plasmodium falciparum involving phosphoethanolamine methylation. Proceedings of the National Academy of Sciences of the United States of America **101**, 6206-6211

8 Salom-Roig, X. J., Hamzé, A., Calas, M. and Vial, H. J. (2005) Dual molecules as new antimalarials. Com. Chem. High T. Scr. **8**, 47-60

9 Vial, H. and Calas, M. (2000) Inhibitors of Phospholipid Metabolism. In Antimalarial Chemotherapy, mechanims of action, modes of resistance, and new directions in drug development (P., R., ed.), pp. 347-365, The Humana Press Inc

10 Vial, H. J., Thuet, M. J., Ancelin, M. L., Philippot, J. R. and Chavis, C. (1984) Phospholipid-Metabolism as a New Target for Malaria Chemotherapy - Mechanism of Action of D-2-Amino-1-Butanol. Biochem. Pharmacol. **33**, 2761-2770

11 Calas, M., Ancelin, M. L., Cordina, G., Portefaix, P., Piquet, G., Vidal-Sailhan, V. and Vial, H. (2000) Antimalarial activity of compounds interfering with Plasmodium falciparum phospholipid metabolism: Comparison between mono- and bisquaternary ammonium salts. J. Med. Chem. **43**, 505-516

12 Ancelin, M. L., Calas, M., Bonhoure, A., Herbute, S. and Vial, H. J. (2003) In vivo antimalarial activities of mono- and bis quaternary ammonium salts interfering with Plasmodium phospholipid metabolism. Antimicrobial Agents and Chemotherapy **47**, 2598-2605

13 Vial, H. J., Wein, S., Farenc, C., Kocken, C., Nicolas, O., Ancelin, M. L., Bressolle, F., Thomas, A. and Calas, M. (2004) Prodrugs of bisthiazolium salts are orally potent antimalarials. Proc. Natl Acad Sci USA **101**, 15458-15463

14 Biagini, G. A., Pasini, E., Hughes, R., De Koning, H. P., Vial, H., O'Neill, P., Ward, S. and Bray, P. (2004) Characterization of the choline carrier of Plasmodium falciparum: a route for the selective delivery of novel antimalarial drugs. Blood Cells **104**

15 Vial, H. J., Thuet, M. J. and Philippot, J. R. (1984) Cholinephosphotransferase and Ethanolaminephosphotransferase Activities in Plasmodium-Knowlesi-Infected Erythrocytes - Their Use as Parasite-Specific Markers. Biochimica Et Biophysica Acta **795**, 372-383

16 Ramirez de Molina, A., Gallego-Ortega, D., Sarmentero-Estrada, J., Lagares, D., Gomez del Pulgar, T., Bandres, E., Garcia-Fontillas, J. and Lacal, J. C. (2008) Choline kinase as a link connecting phospholipid metabolism and cell cycle regulation: Implications in cancer therapy. The International Journal of Biochemistry & Cell Biology **40**, 1753-1763

17 Glunde, K., Jie, C. and Bhujwalla, Z. M. (2004) Molecular causes of the aberrant choline phospholipid metabolism in breast cancer. Cancer Research **64**, 4270-4276

18 Cui, Z. and Houweling, M. (2002) Phosphatidylcholine and cell death. Biochimica Et Biophysica Acta-Molecular and Cell Biology of Lipids **1585**, 87-96

19 Eliyahu, G., Kreizman, T. and Degani, H. (2007) Phosphocholine as a biomarker of breast cancer: Molecular and biochemical studies. International Journal of Cancer **120**, 1721-1730

20 Rodriguez-Gonzalez, A., de Molina, A. R., Fernandez, F., Ramos, M. A., Nunez, M. D., Campos, J. and Lacal, J. C. (2003) Inhibition of choline kinase as a specific cytotoxic strategy in oncogene-transformed cells. Oncogene **22**, 8803-8812

21 Rodriguez-Gonzales, A., de Molina, A. R., Fernandez, F. and Lacal, J. C. (2004) Choline kinase inhibition induces the increase in ceramides resulting in a highly specific and selectives cytotoxic antitumoral strategy as a potential mechanism of action. Oncogene **23**, 8247-8259

22 Banez-Coronel, M., de Molina, A. R., Rodriguez-Gonzalez, A., Sarmentero, J., Ramos, M. A., Garcia-Cabezas, M. A., Garcia-Oroz, L. and Lacal, J. C. (2008) Choline Kinase Alpha Depletion Selectively Kills Tumoral Cells. Current Cancer Drug Targets **8**, 709-719

23 Milanese, L., Espinosa, A., Campos, J. M., Gallo, M. A. and Entrena, A. (2006) Insight into the inhibition of human choline kinase: Homology modeling and molecular dynamics simulations. Chemmedchem **1**, 1216-1228

24 Campos, J., Nunez, M. D., Rodriguez, V., Gallo, M. A. and Espinosa, A. (2000) QSAR of 1,1 '(1,2-ethylenebisbenzyl)bis(4-substitutedpyridinium) dibromides as choline kinase inhibitors: a different approach for antiproliferative drug design. Bioorganic & Medicinal Chemistry Letters **10**, 767-770

25 Campos, J., Nunez, M. C., Conejo-Garcia, A., Sanchez-Martin, R. M., Hernandez-Alcoceba, R., Rodriguez-Gonzalez, A., Lacal, J. C., Gallo, M. A. and Espinosa, A. (2003) QSAR-derived Choline Kinase inhibitors: How rational can antiproliferative drug design be? Current Medicinal Chemistry **10**, 1095-1112

26 Janardhan, S., Srivani, P. and Sastry, G. N. (2006) 2D and 3D quantitative structure-activity relationship studies on a series of bis-pyridinium compounds as choline kinase inhibitors. Qsar & Combinatorial Science **25**, 860-872

27 Nunez, M. C., Conejo-Garcia, A., Sanchez-Martin, R. M., Gallo, M. A., Espinosa, A. and Campos, J. M. (2007) QSAR as a tool for the development of potent antiproliferative agents by inhibition of choline kinase. Current Computer-Aided Drug Design **3**, 297-312

28 Ancelin, M. L. and Vial, H. J. (1986) Several Lines of Evidence Demonstrating That Plasmodium-Falciparum, a Parasitic Organism, Has Distinct Enzymes for the Phosphorylation of Choline and Ethanolamine. Febs Letters **202**, 217-223

29 Choubey, V., Guha, M., Maity, P., Kumar, S., Raghunandan, R., Maulik, P. R., Mitra, K., Halder, U. C. and Bandyopadhyay, U. (2006) Molecular characterization and localization of Plasmodium falciparum choline kinase. Biochimica et Biophysica Acta **1760**, 1027-1038

30 Choubey, V., Maity, P., Guha, M., Kumar, S., Srivastava, K., Kumar Puri, S. and Bandyopadhyay, U. (2007) Inhibition of Plasmodium falciparum Choline Kinase by Hexadecyltrimethylammonium Bromide: a Possible Antimalarial Mechanism. Antimicrob. Agents Ch. **51**, 696-706

31 Aurrecoechea, C., Brestelli, J., Brunk, B. P., Dommer, J., Fischer, S., Gajria, B., Gao, X., Gingle, A., Grant, G., Harb, O. S., Heiges, M., Innamorato, F., Iodice, J., Kissinger, J. C., Kraemer, E., Li, W., Miller, J. A., Nayak, V., Pennington, C., Pinney, D. F., Roos, D. S., Ross, C., Stoeckert, C. J., Treatman, C. and Wang, H. M. (2009) PlasmoDB: a functional genomic database for malaria parasites. Nucleic Acids Research **37**, D539-D543

32 Lambros, C. and Vanderberg, J. P. (1979) Synchronization of Plasmodium-Falciparum Erythrocytic Stages in Culture. Journal of Parasitology **65**, 418-420

33 Bradford, M. M. (1976) A rapid and sensitive method for the quantitation of microgram quantities of protein utilizing the principle of proteindye binding. Anal.Biochem. **72**, 248–254

34 Ancelin, M. L. and Vial, H. J. (1986) Choline Kinase-Activity in Plasmodium-Infected Erythrocytes - Characterization and Utilization as a Parasite-Specific Marker in Malarial Fractionation Studies. Biochimica Et Biophysica Acta **875**, 52-58

35 Aoyama, C., Liao, H. and Ishidate, K. (2004) Structure and function of choline kinase isoforms in mammalian cells. Progress in Lipid Research **43**, 266-281

36 Malito, E., Sekulic, N., Cun See Too, W., Konrad, M. and Lavie, A. (2006) Elucidation of Human Choline Kinase Crystal Structures in Complex with the Products ADP or Phosphocholine. Journal of Molecular Biology **364**, 136-151

37 Yuan, C. and Kent, C. (2004) Identification of critical residues of choline kinase A2 from Caenorhabditis elegans. Journal of Biological Chemistry **279**, 17801-17809

38 Gee, P. and Kent, C. (2003) Multiple isoforms of choline kinase from Caenorhabditis elegans: cloning, expression, purification, and characterization. Biochimica Et Biophysica Acta-Proteins and Proteomics **1648**, 33-42

39 Gibellini, F., Hunter, W. N. and Smith, T. K. (2008) Biochemical characterization of the initial steps of the Kennedy pathway in Trypanosoma brucei: the ethanolamine and choline kinases. Biochemical Journal **415**, 135-144

40 Kim, K. H., Voelker, D. R., Flocco, M. T. and Carman, G. M. (1998) Expression, purification, and characterization of choline kinase, product of the CKI gene from Saccharomyces cerevisiae. Journal of Biological Chemistry **273**, 6844-6852

41 Peisach, D., Gee, P., Kent, C. and Xu, Z. (2003) The Crystal Structure of Choline Kinase Reveals a Eukaryotic Protein Kinase Fold. Structure **11**, 703-713

42 Zlatkine, P., Moll, G., Blais, A., Loiseau, A. and Legrimellec, C. (1993) Transport of Choline by Madin-Darby Canine Kidney-Cells. Biochimica Et Biophysica Acta **1153**, 237-242

43 Hamza, M., Lloveras, J., Ribbes, G., Soula, G. and Dousteblazy, L. (1983) An Invitro Study of Hemicholinium-3 on Phospholipid-Metabolism of Krebs-Ii Ascites-Cells. Biochemical Pharmacology **32**, 1893-1897

44 Cuadrado, A., Carnero, A., Dolfi, F., Jimenez, B. and Lacal, J. C. (1993) Phosphorylcholine - a Novel 2nd Messenger Essential for Mitogenic Activity of Growth-Factors. Oncogene **8**, 2959-2968

45 Lacal, J. C. (2001) Choline kinase: a novel target for antitumor drugs. IDrugs **4**, 419-426

46 Hamze, A., Rubi, E., Arnal, P., Boisbrun, M., Carcel, C., Salom-Roig, X., Maynadier, M., Wein, S., Vial, H. and Calas, M. (2005) Mono- and bis-thiazolium salts have potent antimalarial activity. Journal of Medicinal Chemistry **48**, 3639-3643

47 Kim, K. S., Kim, K. H., Storey, M. K., Voelker, D. R. and Carman, G. M. (1999) Isolation and characterization of the Saccharomyces cerevisiae EKI1 gene encoding ethanolamine kinase. Journal of Biological Chemistry **274**, 14857-14866

48 Lykidis, A., Wang, J., Karim, M. A. and Jackowski, S. (2001) Overexpression of a mammalian ethanolamine-specific kinase accelerates the CDP-ethanolamine pathway. Journal of Biological Chemistry **276**, 2174-2179

TABLE:

Table 1: Kinetic values for recombinant *Pf*CK and *Pf*EK.

Enzyme *Substrate*	K_m (μM)	V_{max} (μmol/min/mg)
PfCK		
choline	135.3 ±15.5	10.76 ±2.81
ethanolamine	>500 mM	62.20 ±3.55
PfEK		
ethanolamine	457.7 ±80.2	1.28 ±0.11
choline	NA	NA

NA for non applicable

FIGURE LEGENDS:

Figure 1: Western immunoblot of *Pf*CK and *Pf*EK

Western blots were revealed with anti-*Pf*CK (A, C) and anti-*Pf*EK (B, D). For A and B: Lane 1, immune serum on non-infected erythrocytes; Lane 2, immune serum on *P. falciparum* lysate; Lane 3, pre-immune serum on *P. falciparum* lysate.

For C and D panels, Western blots were revealed at the three parasite stage development (R: ring; T, trophozoite; S: schizont). Parasite cultures were synchronized and an equal quantity of parasites (10^7 cells) was treated for each stages.

Figure 2: *Pf*CK and *Pf*EK localization

Immunofluorescence assays were done on human red blood cells infected by *P. falciparum* 3D7 strain and revealed by anti-*Pf*CK (A) or anti-*Pf*EK (B) (green). Nuclei were stained in blue with DAPI. Differential interference contrast (DIC) images and merges were presented. Three representative parasitic stages were shown: ring, mature trophozoite and schizont.

Figure 3: Kinetic parameters of *Pf*CK and *Pf*EK

Activity was measured by the formation of phosphocholine or phosphoethanolamine with increasing substrate concentrations (see *Experimental* section). Experiments have been done four times for *Pf*CK and three times for *Pf*EK, each time in duplicate. Representative Michaelis-Menten and Lineweaver-Burk linearization (inserts) plots are shown for *Pf*CK (A), and *Pf*EK (B) enzymes. Activity was expressed as µmol/min/mg. Data were presented as mean ±standard deviation from three measurements.

Figure 4: Inhibition of recombinant *Pf*CK and *Pf*EK

(A) Chemical structures of two commercial compounds, Hemicholinium-3 and 2-amino-1 butanol known to inhibit CK and EK, respectively and of T3 which belongs to the second generation of bis-quaternary ammonium salt. The chemical structure of T3 is a duplicated bis-thiazolium separated by a 12-carbon atom aliphatic chain. This compound is currently under human clinical trials. (B, C) Inhibition curves of *Pf*CK and *Pf*EK. Activities of *Pf*CK (B) and *Pf*EK (C) were measured with increasing concentrations of both specific inhibitors HC-3(Δ), 2-AB(○) and of T3 (■). Activity of both enzymes was giving in percentage of controls. Data are presented as mean ±standard deviation from three measurements. The inhibitor concentrations at 50% activity corresponded to the IC_{50} values (dotted lines).

Figure 5: Inhibition kinetic of *Pf*CK (A) and *Pf*EK (B) by T3 compound

On the left panels, Lineweaver-Burk plots were shown at increasing drug concentrations ; (A) inhibition of *Pf*CK with 0 (Δ), 0.5 (○) and 1 mM (▲) T3 ; (B) inhibition of *Pf*EK 0 (Δ), 0.25 (□) and 0.5 (○) mM T3. Experiments were done twice in triplicate. Data are presented as mean ±standard deviation from three measurements.

On the right panels, (A) for *Pf*CK and (B) for *Pf*EK, the apparent K_m (K_m') were plotted as function of the inhibitor concentration, K_i values were obtained by the value at the intercept with the x-axis as indicated by the arrow (-Ki).

Figure 6: Comparison of *Pf*CK and *P. vivax* EK crystal structures

Superimposition of the Brenner's and Cho/Etn kinase motifs of *Pf*CK (black) and *P. vivax* EK (grey) crystal structures. The insertion containing the tyrosine 329 is not present in *Pv*EK structure. Side-chains of Gln290 (*Pf*CK) and Leu298 (*Pv*EK) residues conserved amongst CK and EK, respectively, are indicated. The position of HC-3 (white) was obtained by the superimposition of the hCKα-2 structure in complex with HC-3. Only HC-3 was let visible. The model suggested that the tyrosine 329 of *Pf*CK (equivalent to Tyr354 in hCKα-2) could interact with HC-3 aromatic ring. The PDB files used were 3FI8 for *Pf*CK, 2QG7 for *Pv*EK and 3FI2 for the hCKα-2 – HC-3 complex. This figure has been done with PyMol software.

Figure 1

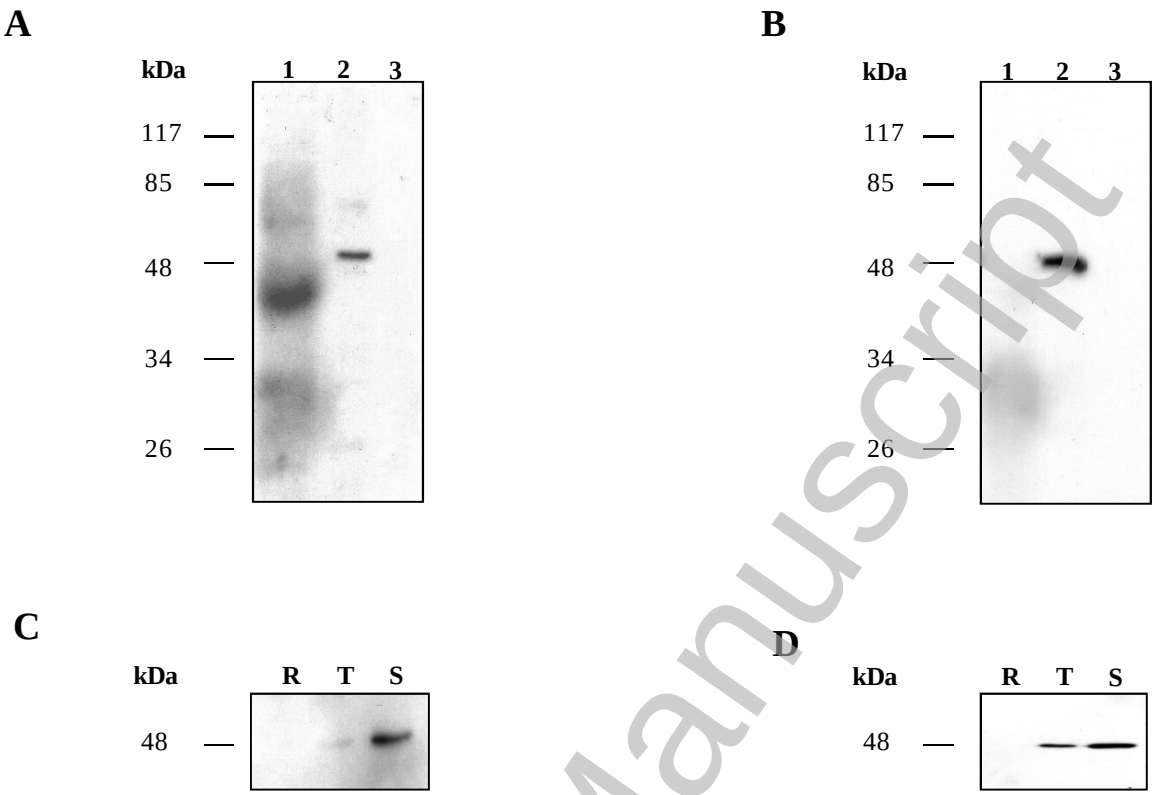

Figure 2

A

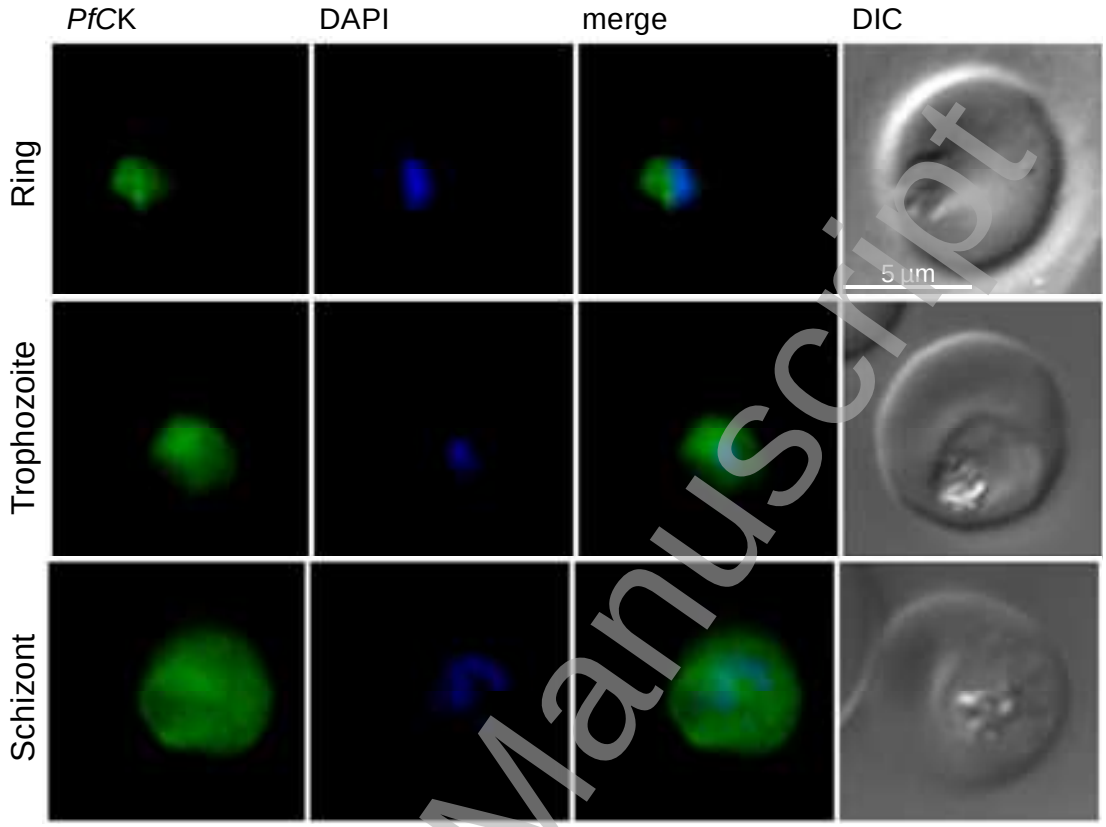

Figure 2

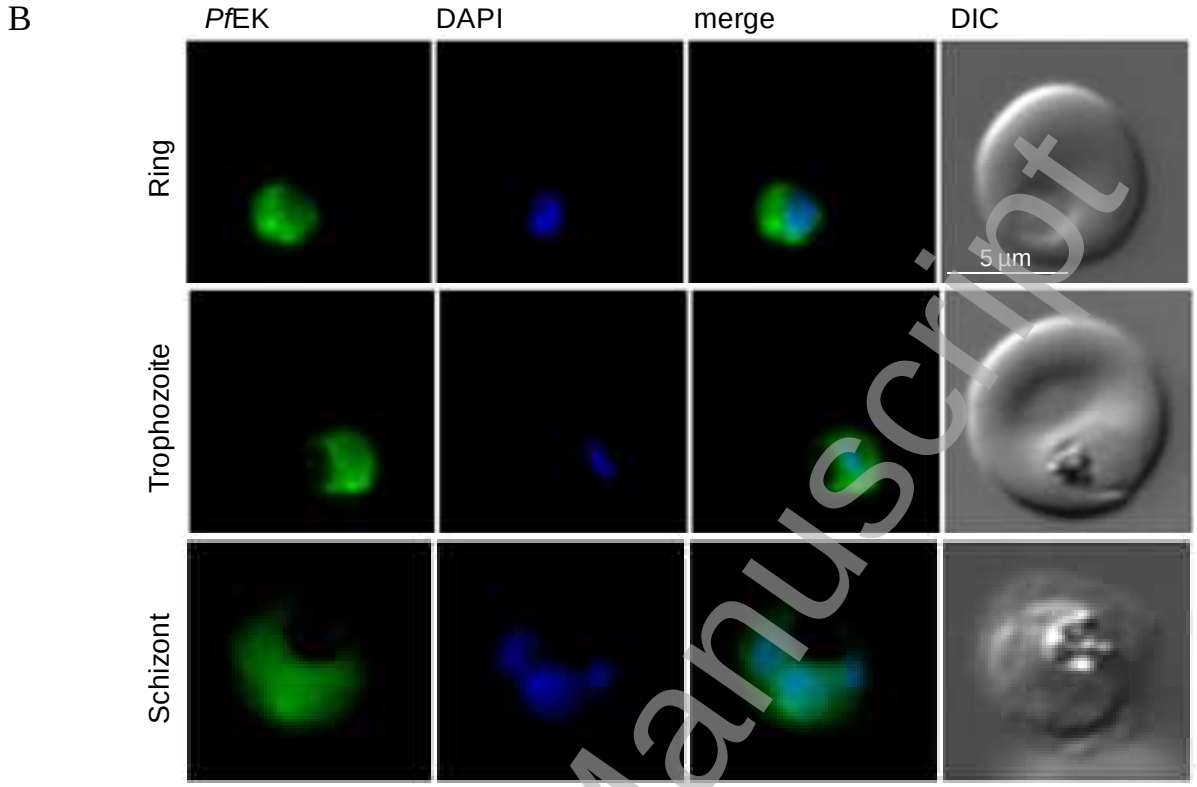

Figure 3

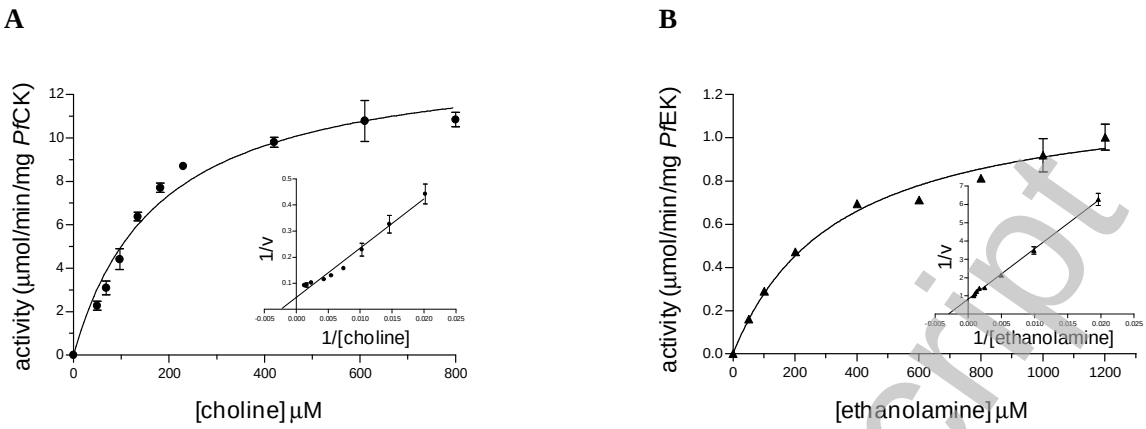

Figure 4

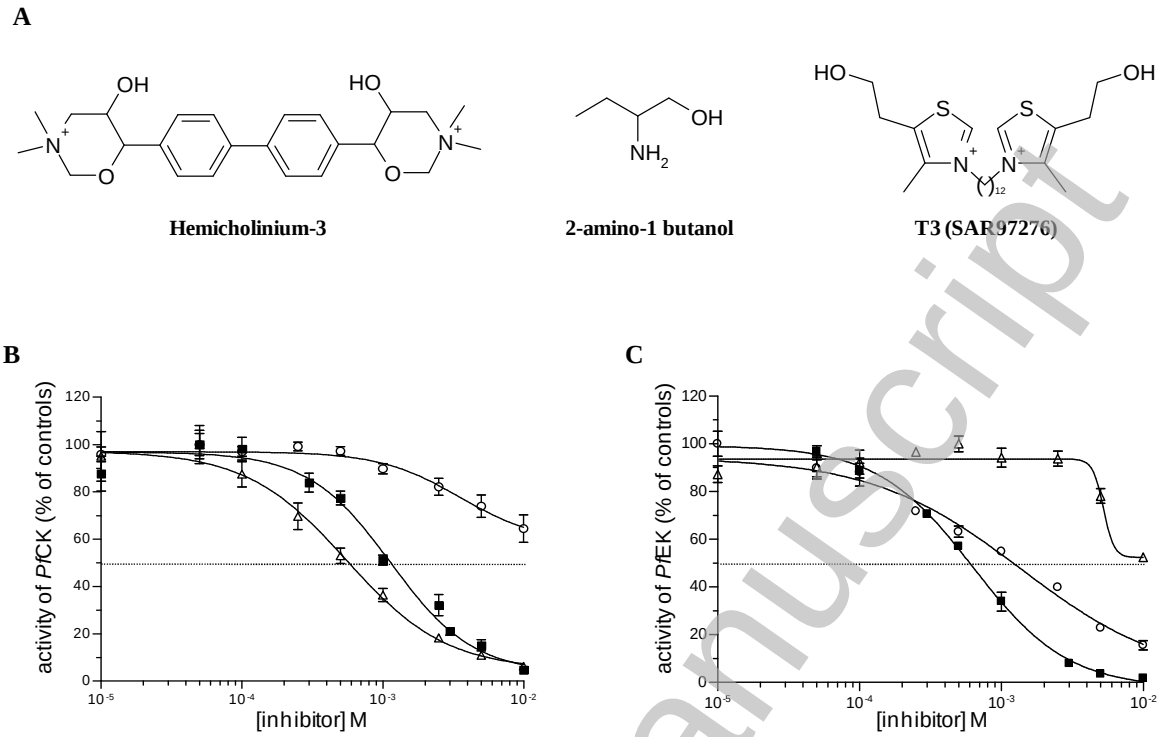

Figure 5

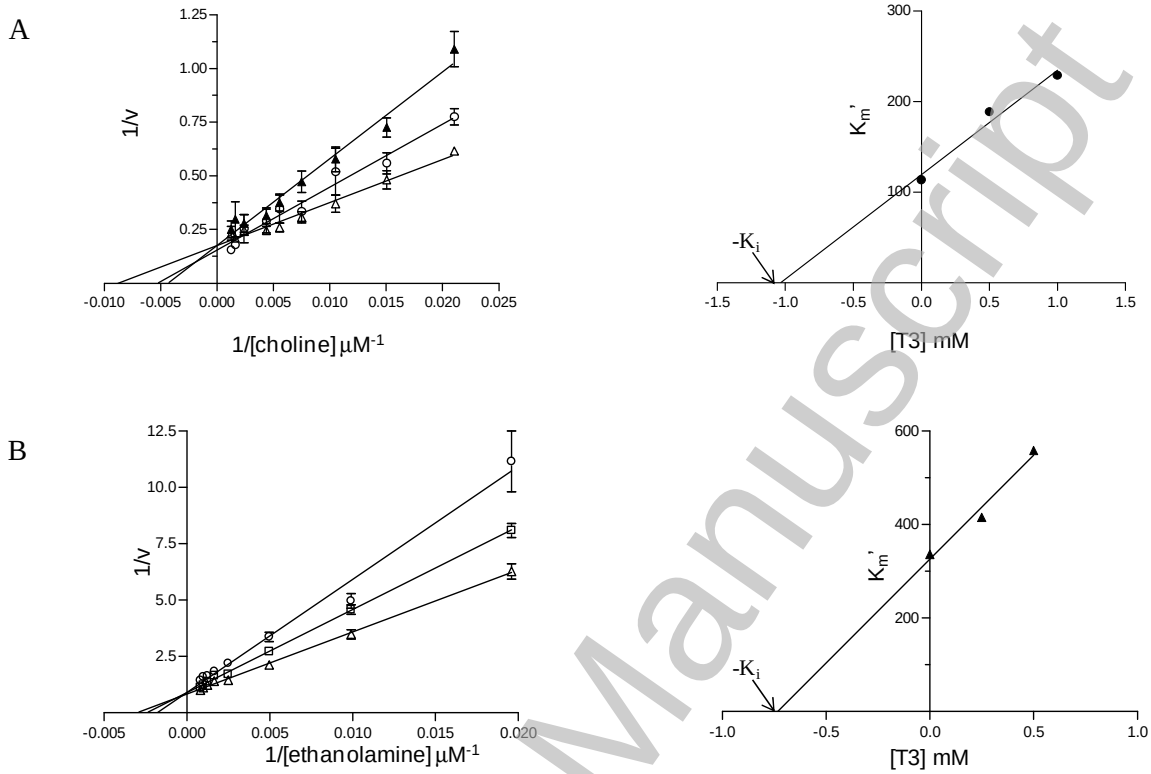

Figure 6